The Astrophysical Journal, 711:389–398, 2010 March 1 doi:10.1088/0004-637X/711/1/389

SDSS J123813.73−033933.0: A CATACLYSMIC VARIABLE EVOLVED BEYOND THE PERIOD MINIMUM

A. Aviles[1], S. Zharikov[1], G. Tovmassian[1], R. Michel[1], M. Tapia[1], M. Roth[2], V. Neustroev[3], C. Zurita[4], M. Andreev[5], A. Sergeev[5], E. Pavlenko[6], V. Tsymbal[7], G. C. Anupama[8], U. S. Kamath[8], and D. K. Sahu[8]
[1] Instituto de Astronomía, Universidad Nacional Autónoma de México, Apartado Postal 877, 22800, Ensenada, BC, Mexico
[2] Las Campanas Observatory, Carnegie Instututio of Washington, Casilla 601, La Serena, Chile
[3] Centre for Astronomy, National University of Ireland, Galway, Newcastle Rd., Galway, Republic of Ireland
[4] Instituto de Astrofisica de Canarias, c/ via Lactea s/n, La Laguna, E38200, Tenerife, Spain
[5] Institute of Astronomy, Russian Academy of Sciences, Terskol, Russia
[6] Crimean Astrophysical Observatory, Nauchny, Ukraine
[7] Tavrian National University, Department of Astronomy, Simferopol, Ukraine
[8] Indian Institute of Astrophysics–CREST, II Block Koramangala, Bangalore 560 034, India
Received 2009 September 12; accepted 2010 January 19; published 2010 February 10

ABSTRACT

We present infrared *JHK* photometry of the cataclysmic variable (CV) SDSS J123813.73−033933.0 and analyze it along with optical spectroscopy, demonstrating that the binary system is most probably comprised of a massive white dwarf with $T_{\rm eff} = 12000 \pm 1000$ K and a brown dwarf of spectral type L4. The inferred system parameters suggest that this system may have evolved beyond the orbital period minimum and is a bounce-back system. SDSS J123813.73−033933.0 stands out among CVs by exhibiting the cyclical variability that Zharikov et al. called brightenings. These are not related to specific orbital phases of the binary system and are fainter than dwarf novae outbursts that usually occur on longer timescales. This phenomenon has not been observed extensively and, thus, is poorly understood. The new time-resolved, multi-longitude photometric observations of SDSS J123813.73−033933.0 allowed us to observe two consecutive brightenings and to determine their recurrence time. The period analysis of all observed brightenings during 2007 suggests a typical timescale that is close to a period of ∼9.3 hr. However, the brightenings modulation is not strictly periodic, possibly maintaining coherence only on timescales of several weeks. The characteristic variability with double orbital frequency that clearly shows up during brightenings is also analyzed. The Doppler mapping of the system shows the permanent presence of a spiral arm pattern in the accretion disk. A simple model is presented to demonstrate that spiral arms in the velocity map appear at the location and phase corresponding to the 2:1 resonance radius and constitute themselves as double-humped light curves. The long-term and short-term variability of this CV is discussed together with the spiral arm structure of an accretion disk in the context of observational effects taking place in bounce-back systems.

Key words: brown dwarfs – novae, cataclysmic variables – stars: dwarf novae – stars: individual (SDSS J123813.73−033933.0)

1. INTRODUCTION

The object cataloged as SDSS J123813.73−033933.0 (hereafter SDSS 1238) was identified with a faint ($r = 17.82$ mag) short-period cataclysmic variable (CV) by Szkody et al. (2003). The optical spectrum of SDSS 1238 shows a blue continuum with broad absorption features originating in the photosphere of a white dwarf (WD) surrounding double-peaked Balmer emission lines, formed in a high inclination accretion disk. The orbital period of the system is $P_{\rm orb} = 0.05592(35)d = 1.34(1)h$, based on spectroscopic data (Zharikov et al. 2006). The orbital period and the spectral features match those of WZ-Sge-type systems, but with this, similarities practically end. A number of observed aspects of the system differ from the majority of short-period CVs. The most intriguing characteristic which we found in this system is a sudden and fast rise in brightness up to ∼0.45 mag during a short time, of about half of the orbital period. After reaching its peak, the brightness slowly decreases, lasting ∼3–4 hr, down to the quiescence level. We call these events brightenings in order to distinguish them from the more common outbursts, humps, flickering, and other types of variability documented in short-period CVs. These brightenings seemed to happen cyclically about every 8–12 hr. In addition to brightenings, a nearly permanent sinusoidal variability was detected in the light curve of SDSS 1238 with a period half that of the spectroscopic orbital period $P = P_{\rm orb}/2 = 40.25$ minutes (hereafter, the double-humped light curve). The amplitude of the double-hump variability depends on the phase of the brightenings. It increases with a total rise in brightness of up to ∼0.2 mag and decreases until it almost disappears during the quiescence (Zharikov et al. 2006). A similar behavior was found later by Szkody et al. (2006) in another short-period CV, SDSS J080434.20+510349.2 (hereafter SDSS 0804) which has an identical spectral appearance to SDSS 1238 in quiescence. Zharikov et al. (2006, 2008) advanced the hypothesis that the double-humped light curve is a signature of 2:1 resonance in the accretion disks of these systems. In order for the accretion disk to reach permanently the 2:1 resonance radius, the mass ratio of the binary component must be extreme ($q \leqslant 0.1$), and as such these objects could qualify as bounce-back systems, e.g., CVs, which are old enough to reach the period minimum and leap toward slightly longer orbital periods, as predicted by Paczynski (1981). It is supposed that accretion disks of WZ-Sge systems reach 2:1 resonance radius during superoutburst, when some of them have been noted to show double-humped light curves (Patterson et al. 2002b). The superoutbursts of WZ-Sge-type systems are infrequent and happen every two dozen or more years. Oddly enough, SDSS 0804 went into the superoutburst in 2006 (Pavlenko et al. 2007) and exhibited all necessary attributes of a classical WZ-Sge-type object. Regrettably, the brightenings disappeared from the light curves of SDSS 0804 after the superoutburst, although the double-hump light curve persists (Zharikov

et al. 2008). Thus, the SDSS 1238 remains the only object that still shows brightenings. Intrigued by the new photometric phenomenon observed in these two systems, we conducted a new time-resolved photometric study of SDSS 1238 to establish the reasons behind their common nature, and to understand the origin of the cyclic brightenings and their relation to the amplitude of the double-humped light curve. Meanwhile, we discovered that SDSS 1238 was marginally detected as an infrared source by Two Micron All Sky Survey (2MASS), and secured accurate near-IR photometry of the object. In Section 2, we describe our observations and data reductions. The data analyses and the results are presented in Sections 3–5, while a general discussion and conclusions are given in Section 6.

2. OBSERVATIONS AND DATA REDUCTION

The object is listed in the 2MASS[9] Point Source Catalogue with $J = 16.65(13)$, $H = 16.49(23)$, $K \sim 16.42$ mag. These magnitudes are close to the detection limits of 2MASS, particularly in the K band. In order to have more accurate photometry, we obtained new observations of SDSS J123813.73−033933.0 in JHK_s on 2009 June 17 with the near-infrared camera PANIC (Martini et al. 2004) attached to the 6.5 m Baade/Magellan Telescope at Las Campanas Observatory (LCO). PANIC provides an image scale of $0\farcs125$ pixel^{-1} on a Hawaii HgCdTe 1024×1024 array detector. The FWHM of the point-spread function was between $0\farcs55$ and $0\farcs60$ during our observations. For each filter, nine dithered frames spaced by $10''$ were taken, with total on-source integration times of 540 s in each of the three filters. The nine frames were shifted and averaged to produce the final images. Standard sky-subtraction and flat-field correction procedures were applied. Aperture ($1\farcs2$) photometry was performed with DAOPHOT within IRAF[10] in the standard way. Flux calibration was performed using standard stars SJ 9146 and SJ 9157 from the list of Persson et al. (1998) and the total errors are estimated to be less than 0.05 mag. The resulting magnitudes of SDSS 1238 are $J = 17.07(5)$, $H = 16.65(5)$, and $K = 16.42(5)$ and corresponding colors $J - H = 0.42$, $H - K_s = 0.23$, and $J - K_s = 0.65$.

In order to investigate whether flux variations in the near-IR occur in this system in timescales of a few minutes, we measured the J, H, and K_s fluxes from each of the nine short-exposure (60 s) frames in each filter. In the ∼15 minutes that each series lasted, we did not detect any variability within the ∼0.15 mag photometric uncertainty associated with each single frame. Note that in longer timescales (comparable to the orbital period), the system is expected to show some variability in the near-IR, mostly due to the elliptical shape of Roche-lobe filling secondary, but these could be missed in a 15 minute time series. The ellipsoidal variability of the secondary can be calculated and it has been taken into account in further considerations of IR magnitudes.

The objective of our optical photometry of SDSS 1238 was to study the phenomenon of brightenings. Taking into account the long duration of the brightenings and the uncertainty of the cycle period (Zharikov et al. 2006), we planned and executed a multi-longitude observational campaign of this object. Time-resolved CCD photometry was obtained at several facilities: the 1.5 m telescope at the Observatorio Astronómico Nacional at San Pedro Mártir (SPM) in Mexico; the 0.8 m IAC80 telescope at the Observatorio del Teide in the Canary Islands, Spain; the 2.1 m telescope at the Bohyunsan Optical Astronomy Observatory (BOAO) in South Korea; the 2 m telescope at the Terskol Astrophysical Observatory in the Northern Caucasus, Russia; and the 2 m Himalayan Chandra Telescope of the Indian Astronomical Observatory (IAO), Hanle, India. The data reduction was performed using both ESO-MIDAS and IRAF software. The images were bias-corrected and flat-fielded before aperture photometry was carried out. The log of photometric observations is presented in Table 1.

The long-slit observations have been obtained with the Boller and Chivens spectrograph[11] on the 2.1 m telescope at the SPM site with a resolution of 3.03 Å pixel^{-1}. The spectra span the wavelength range 4000–7100 Å. In order to improve the signal-to-noise ratio, we obtained a series of phase-locked spectra: 10 spectra were taken at equal phase intervals over a single orbital period $P_{\rm orb} = 80.5$ minutes with an exposure time of 486 s per spectrum. This sequence of spectra was repeated at exactly the same phase intervals for subsequent periods and subsequent nights. This allows us to calculate the phase-averaged spectra, summarizing the spectra of the same orbital phase obtained during one night and the whole set of observations without further decreasing the time resolution. The log of spectroscopic observations is presented in Table 2.

3. SPECTRAL ENERGY DISTRIBUTION: SYSTEM PARAMETERS AND DISTANCE TO THE OBJECT

The spectral energy distribution (SED) of the object in the range of 4000–25000 Å is shown in Figure 1. The detailed description of the SDSS 1238 optical spectrum was given in our previous paper (Zharikov et al. 2006). The overall appearance of the spectrum has not changed, but we detect a significant variability of the equivalent widths of Balmer emission lines from epoch to epoch. The Balmer lines are about two times weaker in the 2009 observations compared to the 2004 spectra (Figure 2). The continuum, however, has not changed during the last five years, as we compare V-band magnitudes in quiescence between brightenings. The average quiescence magnitude[12] between brightenings remains constant at around $V \cong 17.8 \pm 0.1$.

The present near-IR measurements demonstrated that there is significant IR excess emission to that expected from the Rayleigh–Jeans tail of the optical spectrum for a WD. In fact, neither a WD nor a power-law flux from the accretion disk, nor their combination, can explain the observed IR excess. The most probable source of IR excess is the radiation from the secondary star. To determine the spectral type of the secondary and the distance to the system, we fitted the observed optical–infrared SED of the object with a simple model: the total flux $F^*(\lambda)$ is the sum of contributions from a WD with a hydrogen atmosphere, $F_{\rm WD}(T_{\rm eff}, \lambda)$ (DA type WDs), an accretion disk with $F_{\rm AD} \sim \lambda^{-\frac{7}{3}}$ (Lynden-Bell 1969), and a red/brown dwarf with $F_{\rm BD}(\lambda)$:

$$F^*(\lambda) = F_{\rm WD}(T_{\rm eff}, \lambda) + F_{\rm AD}(\lambda) + F_{\rm BD}^{\rm SpT}(\lambda). \quad (1)$$

Brown dwarf fluxes were taken from the literature (McLean et al. 2003, 2007) and online sources.[13] The WD spectra with

[9] http://www.ipac.caltech.edu/2mass/

[10] IRAF is distributed by the National Optical Astronomy Observatory, which is operated by the Association of Universities for Research in Astronomy, Inc., under cooperative agreement with the National Science Foundation.

[11] http://www.astrossp.unam.mx

[12] Secondary photometric standards were established in the field of SDSS 1238, by calibrating them using reference star S2003313360 from GSC-II http://www.gsss.stsci.edu/Catalogs/GCS/GSC2/GSC2.html

[13] See http://web.mit.edu/ajb/www/browndwarfs/

Table 1
Log of Time-resolved Observations of SDSS J123813.73−033933.0 in the *V* Band

Date	HJD Start+ 2454000	Telescope	Exp. Time Number of Integrations	Duration
Photometry				
2007 Feb 25	156.832	1.5 m/SPM/México	120 s × 160	5.3 hr
2007 Feb 26	157.845	1.5 m/SPM/México	120 s × 144	4.8 hr
2007 Mar 15	174.756	1.5 m/SPM/México	220 s × 95	5.8 hr
2007 Mar 18	177.767	1.5 m/SPM/México	170 s × 91	4.3 hr
2007 Mar 19	178.716	1.5 m/SPM/México	240 s × 108	7.2 hr
2007 Mar 20	179.414	2 m/Terksol/Russia	120 s × 118	3.9 hr
2007 Mar 20	179.746	1.5 m/SPM/México	160 s × 77	3.4 hr
2007 Mar 20	180.290	2 m/Terksol/Russia	120 s × 152	5.1 hr
2007 Mar 21	181.169	2 m/IAO/India	120 s × 135	7.5 hr
2007 Mar 21	181.286	2 m/Terksol/Russia	120 s × 210	7 hr
2007 Mar 22	182.164	2 m/IAO/India	120 s × 198	6.9 hr
2007 Mar 22	182.302	2 m/Terksol/Russia	120 s × 195	6.5 hr
2007 Mar 22	182.435	0.8 m.IAC80/Spain	270 s × 98	7.4 hr
2007 Mar 25	185.032	2.1 m/BOAO/Korea	135 s × 107	4.0 hr
2007 Apr 25	216.696	0.8 m/IAC80/Spain	200 s × 101	5.6 hr
2007 Apr 27	218.648	0.8 m/IAC80/Spain	200 s × 116	6.4 hr
2008 Mar 9	535.904	1.5 m/SPM/México	60 s × 150	2.5 hr
2008 Mar 10	536.882	1.5 m/SPM/México	60 s × 200	3.3 hr
2008 Mar 11	537.889	1.5 m/SPM/México	60 s × 170	2.8 hr
2009 Feb 27	890.826	1.5 m/SPM/México	60 s × 184	3.1 hr
2009 Feb 28	891.814	1.5 m/SPM/México	60 s × 227	3.8 hr
2009 Mar 1	892.851	1.5 m/SPM/México	60 s × 218	3.6 hr

Table 2
Log of Time-resolved Spectroscopic Observations of SDSS J123813.73−033933.0

Date	HJD Start+ 2454000	Telescope	Exp. Time Number of Integrations	Duration
Spectroscopy				
2009 Jan 24	855.99	2.1 m/SPM/México	486 s × 7	0.52 hr
2009 Jan 25	856.96	2.1 m/SPM/México	486 s × 17	2.43 hr
2009 Jan 26	857.90	2.1 m/SPM/México	486 s × 20	2.69 hr
2009 Jan 27	856.96	2.1 m/SPM/México	486 s × 10	1.2 hr

a mass range of $M_{\rm WD} = 0.6$–$1.1\ M_\odot$ were used with a $0.1\ M_\odot$ step and the radii were calculated using the WD radius–mass relation of

$$R_{\rm WD} = 1.12 \times 10^9 \left(1 - \frac{M_{\rm WD}}{1.44\ M_\odot}\right)^{\frac{3}{5}}$$

from Nauenberg (1972) and Warner (1995). Spectra of WDs in the 4000–25000 Å range with pure hydrogen atmosphere were obtained using ATLAS9 (Kurucz 1993) and SYNTH (Piskunov 1992) codes for an appropriate range of temperatures. Although our previous temperature estimate was $T_{\rm WD} = 15{,}600 \pm 1000$ K based on fits to the absorption portion of Balmer lines (Zharikov et al. 2006), in the present fitting procedure we allowed a wider temperature range from $T_{\rm eff} = 11{,}000$ to 18,000 K, because of the larger number of free parameters. The calculations were performed with a 1000 K step and with the surface gravity $g = \gamma \frac{M_{\rm WD}}{R^2_{\rm WD}}$. The spectra are normalized to $\lambda_0 = 5500$ Å and the contribution of the WD is

$$F_{\rm WD}(T_{\rm eff}, \lambda) = C_1(\delta) * F^{\rm norm}_{\rm WD}(T_{\rm eff}, \lambda),$$

where $C_1(\delta) = 10^{-0.4*(V+\delta+M^0_V)}$, $V = 17.8$ is the object's magnitude in quiescence, and δ is a parameter, determining the contribution of the flux from the WD in the *V* band. Finally, the $M^0_V = 21.109$ is the constant to convert magnitudes into flux (in erg cm^{-2} s^{-1} Å^{-1}) in the *V* band. The spectrum of the accretion disk was assumed to be a simple power law

$$F_{\rm AD}(\lambda) = (C_1(0) - C_1(\delta)) \times \left(\frac{\lambda}{\lambda_0}\right)^{-\frac{7}{3}},$$

where $(C_1(0) - C_1(\delta))$ determines the contribution from the accretion disk in the *V* band, assuming that the WD and the accretion disk are the only contributors in that wavelength as the only other contributor is the brown dwarf, which has a negligible flux in *V*.

The distance to the object is estimated to be

$$d = R_{\rm WD} \sqrt{\frac{F^{\rm bb}(T_{\rm eff}, 5500\ \text{Å})}{F_{\rm WD}(5500\ \text{Å})}},$$

where $F^{\rm bb}(T_{\rm eff}; 5500\ \text{Å})$ is the blackbody flux at $\lambda = 5500$ Å with effective temperature $T_{\rm eff}$.

Observed SEDs of red/brown dwarfs of spectral types between M6 and L5 normalized to fit the observed flux in *J* were used. The bolometric correction to the *J* magnitude for each spectral type was taken from Tinney et al. (2003).

The free parameters of the three-component model are the WD effective temperature, $T_{\rm eff}$, the mass of the WD, $M_{\rm WD}$, the spectral type of the secondary star, SpT, and the parameter δ (in magnitudes). The best-fit model to the observed SDSS 1238

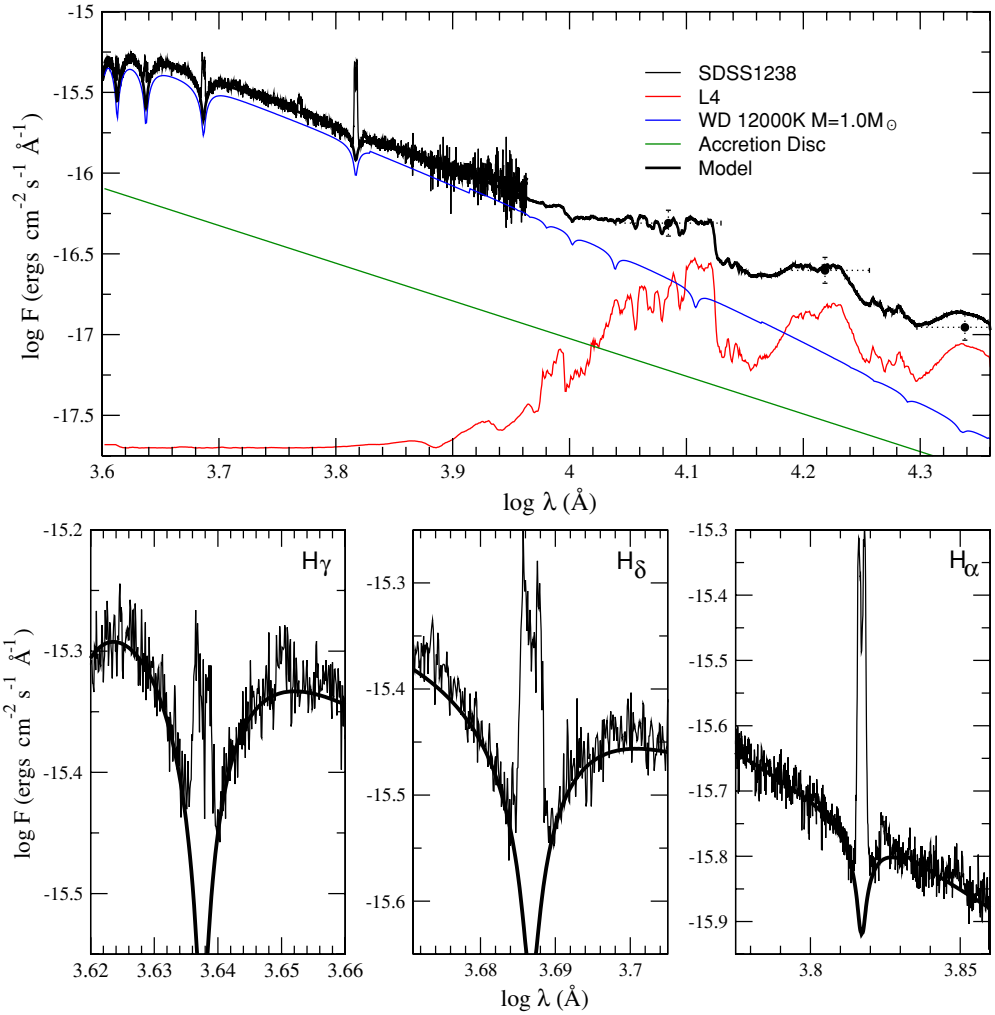

Figure 1. Spectral energy distribution of SDSS 1238 and the result of the model fit (top). Spectrum fragments around H_γ, H_δ, and H_α lines are shown in bottom panels.

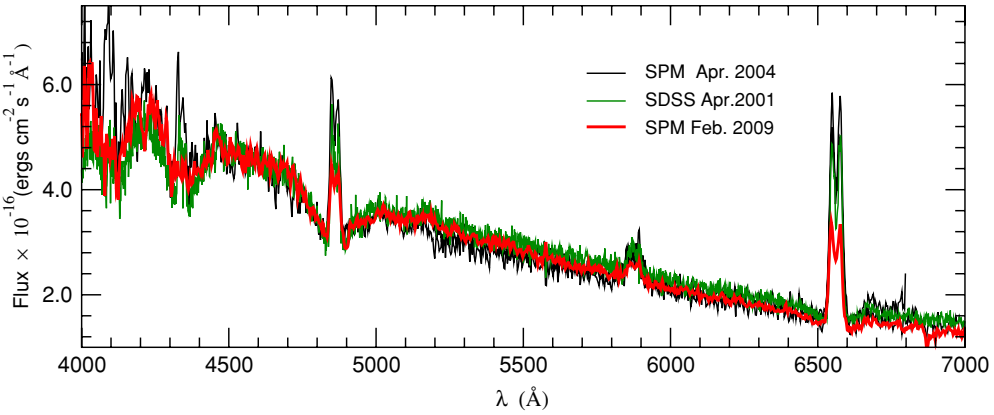

Figure 2. Low-resolution time-average spectra of SDSS1238 obtained in different epochs.

spectrum in the 0.4–2.5 μm range achieved for the following set of parameters (Figure 1) is $T_{\rm WD} = 12{,}000$ K, SpT = L4, $M_{\rm WD} = 1.0\,M_\odot$, and $\delta = 0.1$. The deduced distance to the object is 110 pc. We studied the behavior of χ^2 versus a single fit parameter, when the other three are fixed to their corresponding best values. Figure 3 presents χ^2 plots for various parameters with marked confidence levels corresponding to 95%, 80%, and 60%. We can state that χ^2 tends to the minimum value always, when $T_{\rm WD} = 12{,}000$ K and $\delta = 0.05$–0.15 regardless of the value of the other parameters. At the same time, there is a dependence between the mass of the WD and the spectral type of the secondary: the lower the mass, the larger the radius of WD, and thus, the larger the distance to the system, resulting in an earlier spectral type of the secondary. The best fit to the optical part of the spectrum is reached with the mass of the WD of $M_{\rm WD} = 1.0\,M_\odot$, leading to the cited distance of 110 pc, and spectral type of the secondary, L4. The entire range of secondary from SpT = M9 at $M_{\rm WD} = 0.6\,M_\odot$ and $d = 160$ pc to SpT = L4 at $M_{\rm WD} = 1.0\,M_\odot$, $d = 110$ pc was considered. However, a pronounced minimum in χ^2 for

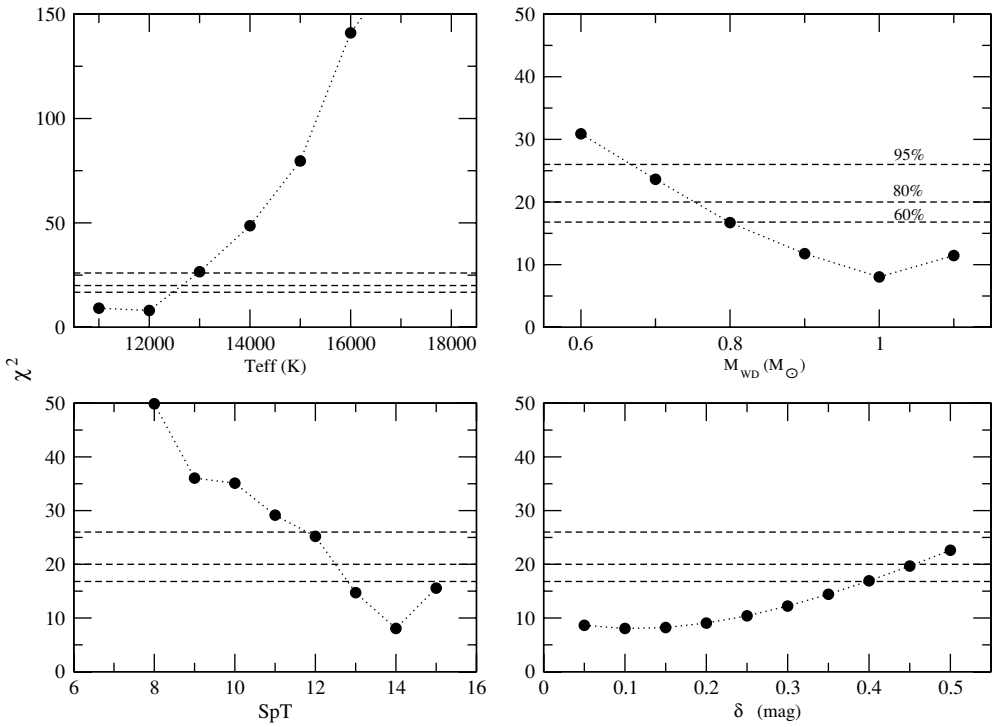

Figure 3. χ^2 vs. parameters of the fit, where $T_{\rm eff}$ is an effective temperature of the primary WD, $M_{\rm WD}$ is a mass of the WD, SpT is a spectral type of the secondary (from M6V/SpT = 6 to L6/SpT = 16), and δ is a ratio between accretion disk and WD contribution in the continuum flux of the SDSS1238 in the V band. The formal confidence levels by the fit are presented by dashed lines. The numbers at the dashed lines are a probability to reject a model with χ^2 above corresponding line.

rather massive WD strongly suggests the presence of a brown dwarf in this system. The indication of a massive WD is not accidental; a CV with a brown dwarf secondary, supposed to have evolved beyond minimum orbital period limit, has an age ∼3–5 × 10^9 years and a long history of accretion. A priori, the bounce-back CVs are assumed to harbor a massive WD, although the distribution of known masses of all WDs in eclipsing systems does not show any trend (Knigge 2006). But when considering only the short-period end of that distribution as Littlefair et al. (2008) did, then it becomes apparent that evolved systems systematically have more massive WDs. The upper limit for the mass of the secondary is $M_{\rm BD} \leqslant 0.09\,M_\odot$ for SpT = M9 or $M_{\rm BD} \leqslant 0.07\,M_\odot$ for SpT = L4 (Close et al. 2003). But it is also a well-known fact that the secondaries of CVs tend to show systematically an earlier spectral class and a larger radius with secondaries of lower mass than the corresponding single stars on the main sequence (Littlefair et al. 2008). So we expect that the mass of the secondary in SDSS 1238 hovers around the lower edge of the above-mentioned range of masses.

Note that due to the high galactic latitude of this object ($b = 59.5$) and the inferred small distance, the interstellar extinction is negligible. We also would like to emphasize that in the above calculations we took into account the fact that the state of the system was unknown at the moment of acquiring the IR data. Therefore, we conducted the fitting for both cases, considering that the system might have been at the maximum of the brightenings during the IR observations or at the bottom. That introduced only a minor change, basically decreasing the distance to the system by ∼15 pc and not affecting our conclusions regarding the spectral type of the secondary. Finally, we would like to comment on the discrepancy in the temperature determination of the WD, which is larger than we would like as compared to that of Zharikov et al. (2006). In the latter, the temperature and gravity could not be determined simultaneously, and one parameter had to be fixed in order to calculate the other, which always introduces ambiguity, as neither of these two parameters could be estimated independently. In this paper, we take a more complex approach: not only profiles of the lines are being fitted, but the continuum is taken into consideration as well. Also, the presence of the secondary adds additional restraints on the distance and, thus, on the size of the WD. The SED of the accretion disk, which may not necessarily obey the canonical power-law index, is the source of the largest uncertainty in our analysis. Since the contribution of the disk is limited to only ⩽20%, so is the accuracy of our estimates. With all that in mind, we still end up with a range of spectral classes for the secondary that implies that SDSS 1238 is a bounce-back system.

4. DOPPLER TOMOGRAPHY OF SDSS 1238

The H_α emission line originating in the accretion disk is the least affected by the absorption from the underlying WD. Therefore, we constructed Doppler maps (Marsh & Horne 1988) of H_α using all our data obtained in 2004 and 2009 (Figure 4, top). The individual maps of separate nights resemble each other so much that combining all available data did not smooth out details, but made them much more convincing. In order to overplot contours of the secondary star, the location of the WD, the trajectory of the stream, and resonance radius of the disk, we used the best-fit parameters to the SED (see previous section). Thus, the WD mass of $M_{\rm WD} = 1.0\,M_\odot$ was adopted. Due to the ambiguity in determining precise masses of brown dwarfs, we adopted a mass ratio of $q = 0.05$. This value is typical for systems considered as bounce-back (Knigge 2006) and it is the same mass ratio which was obtained for SDSS 0804, a twin of SDSS 1238, from the super-hump period observed

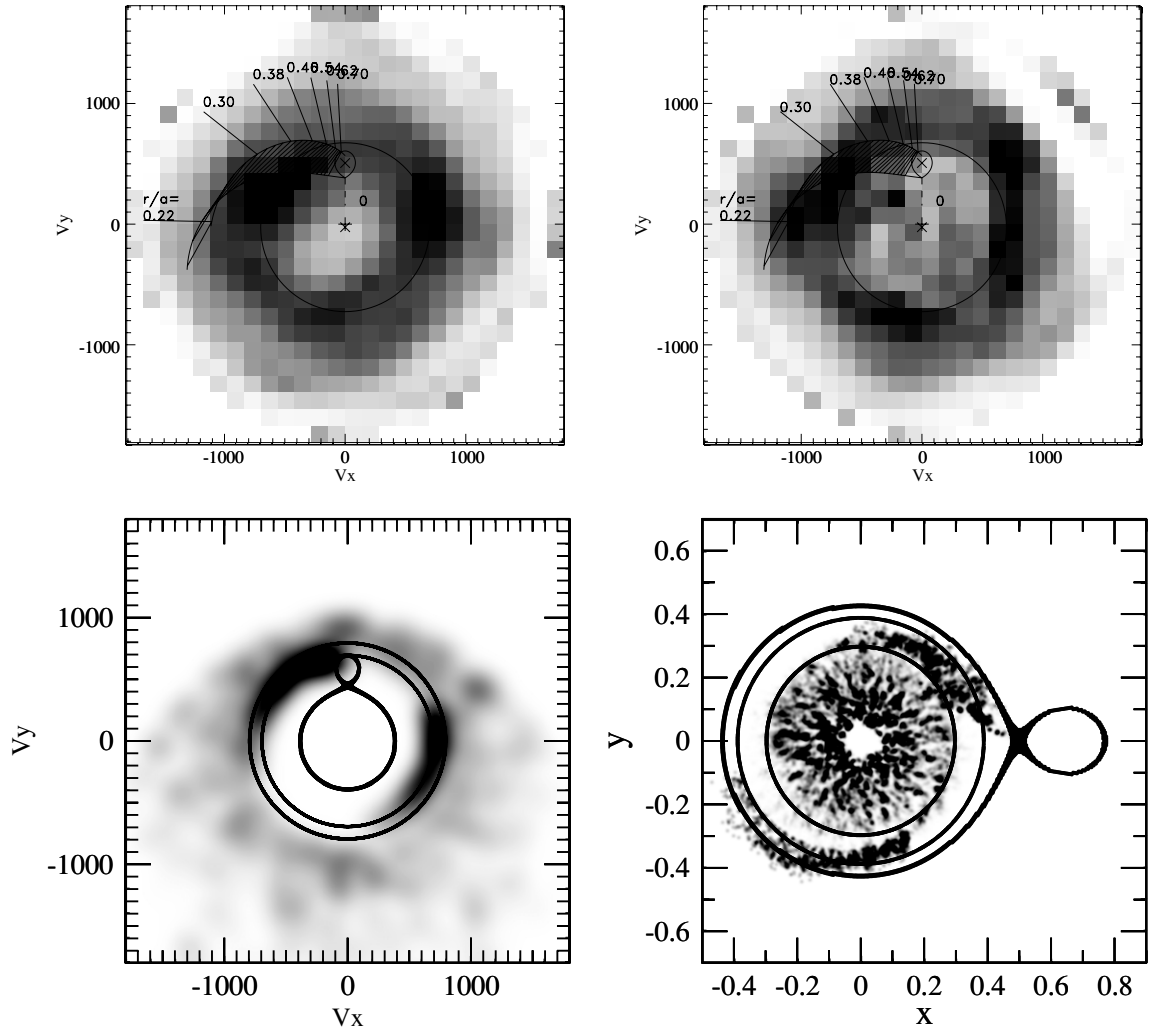

Figure 4. Top: H_α Doppler maps constructed on all data obtained in the 2004 (left) and 2009 (right) yy. The circle show the velocity at 2:1 resonance radius. Bottom: the synthetic Doppler map (left) obtained from a model accretion disk (right) for the system with $M_{WD} = 1.0\,M_\odot$ and $q = 0.05$. The circles correspond to 2:1 and 3:1 resonance radii.

during the superoutburst in 2006 (Pavlenko et al. 2007; Zharikov et al. 2008). Before SDSS 0804 underwent a WZ-Sge-type superoutburst, it showed similar peculiar photometric variability to SDSS 1238. In addition, it shares every other characteristic of a WZ-Sge-type object, and was also proposed as a candidate to the bounce-back system (Zharikov et al. 2008).

As already noted, the structure of the accretion disk did not change between the two epochs of our observations. There is a bright spot at the expected place where the stream of matter from the secondary collides with the accretion disk, but it overlaps with a much larger and prolonged structure, too extended to be a part of the spot. Another extended bright region of similar size can be seen at velocity coordinates ($\approx$700 km s^{-1}, $\approx$0 km s^{-1}) as well as a less bright structure at (≈ -200 km s^{-1}, ≈ -800 km s^{-1}). Similar Doppler maps were obtained for WZ-Sge during superoutburst in 2001 (Baba et al. 2002; Howell et al. 2003; Steeghs 2004) and in quiescence for bounce-back candidates SDSS 1035 (Southworth et al. 2006) and SDSS 0804 (A. Aviles et al. 2010, in preparation).

Such brightness distribution in the Doppler map can be interpreted as evidence of spiral waves in the disk (see, for example, Steeghs & Stehle 1999; Steeghs 2001, and references therein). The formation of a spiral structure in an accretion disk of a close binary system was predicted by Lin & Papaloizou (1979) and explored by various authors (Matsuda et al. 1990; Heemskerk 1994; Stehle 1999; Kunze & Speith 2005; Truss 2007, and references therein). Sawada et al. (1986a, 1986b) demonstrated from high-resolution numerical calculations that spirals will always be formed in accretion disks under tidal forces from the secondary. They actually used $q = 1$ in their models, but observationally, such spirals were detected in a number of systems only during outbursts of dwarf novae (DNe). The careful examination of quiescent disks of the same systems did not reveal any spiral structures in longer period DNe. Steeghs & Stehle (1999) argued that little evidence of spiral arms in the emission lines is expected in systems with low values of viscosity.

On the other hand, spiral arms related to 2:1 resonance can be found in systems with extremely low mass ratio $q < 0.1$ as originally was predicted by Lin & Papaloizou (1979). The bounce-back systems and, related to them, WZ-Sge stars, are examples of such objects. The long outburst recurrence time in WZ-Sge systems is probably explained by a very low viscosity in their accretion disks, yet spiral arms can be observed permanently in quiescent bounce-back systems in which on one side there is a massive WD, which gained mass during a long accretion history, and on another side there is a late-type brown dwarf, providing a mass ratio of $\leqslant$0.06. Figure 4 (bottom,

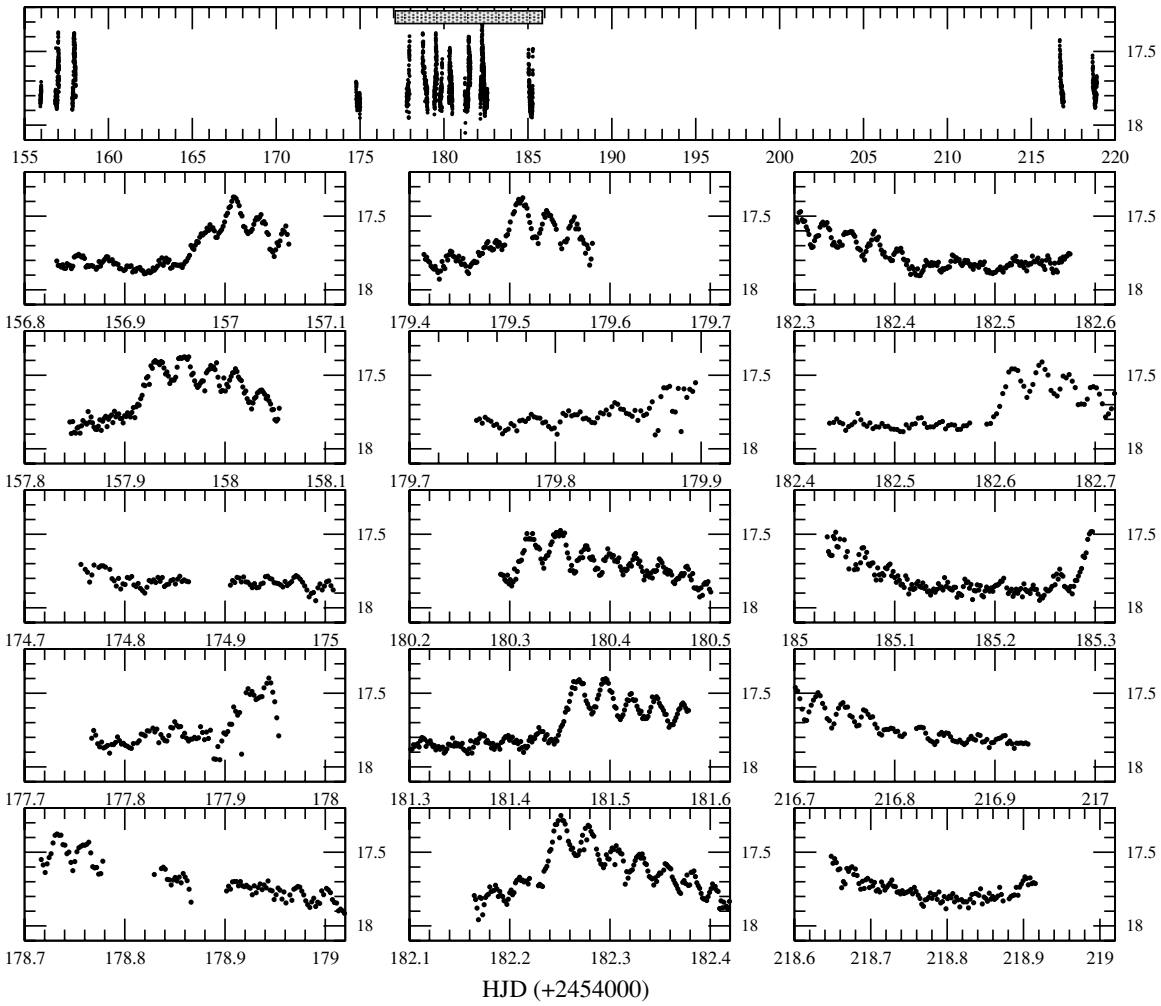

Figure 5. Light curve of SDSS 1238 in the *V* band obtained in the 2007 year. Each night is presented in a separate panel.

left) depicts a synthetic Doppler map constructed from a model accretion disk that is shown on the bottom right panel. The latter was calculated with the binary system parameters derived above by using smooth particle hydrodynamics according to Murray (1996), Kunze et al. (1997), and references therein. The artificial Doppler map reproduces the observed map in a case when there is a brightness excess within spiral arms. Most of the disk particles are on periodic orbits, which are most favorable from the point of view of viscosity. However, the resonance dispatches some particles onto aperiodic orbits creating viscosity perturbations, which will create excess of heat. A slightly different interpretation of spiral arm brightness is offered by Ogilvie (2002). The mechanism is not very well established, but it is natural to assume that in these regions there will be excess emission.

5. CYCLIC BRIGHTENINGS

Figure 5 displays the light curve of SDSS 1238 obtained in 2007. In general, the object shows an identical behavior to previous years, as described by Zharikov et al. (2006). There are two distinct types of variability: a long-term variability (LTV), lasting more than 8 hr, and a short-term variability with a period corresponding to half the orbital period. Follow-up observations during 2008 and 2009 confirm a steady presence of both types of variability in the light curve (Figure 6). Continuous observations during about 15 hr obtained on 2007 March 22 (HJD 2454182.15−2544182.60, Figure 7) allowed us to observe two consecutive brightenings and, thus to determine their recurrence time directly (∼9 hr). Zharikov et al. (2006) demonstrated that brightenings occurred cyclically with periods in between 8 and 12 hr; however, it was not possible to establish if the phenomenon was strictly periodic or not. Armed with more data, and the advantage of detecting consecutive events by employing multi-longitude observations, we performed a simple period search. The period analysis of all data obtained during 2007, based on a discrete Fourier transform method (Deeming 1975), results in a strong peak at a frequency $f_{\rm LTV} = 2.59$ day^{-1} with FWHM of 0.1. This conforms with the period of $P_{\rm LTV} = 9.28 \pm 0.36$ hr $\approx 7 P_{\rm orb}$ (Figure 8). However, the data folded with this period look messy because, apparently, some re-brightenings happen with a different cycle period. It shows that the large uncertainty in the period value is not just a result of a scarce amount of data, or its uneven distribution, but that the brightenings are not strictly periodic in long timescales. The peak $2 \times f_{\rm orb} = 35.76$ day^{-1}, corresponding to the half of the orbital period, $P_{\rm orb}/2 = 40.3$ minutes, is also present in the power spectrum. There are some additional peaks which are 1-day aliases or a combination of high harmonics of $f_{\rm LTV}$ with $2 \times f_{\rm orb}$. We have repeated the same analysis for the data obtained only within HJD 2454177.1−2544185.6, when we observed the object with small observational gaps. The result of the analysis of periodicity for this selection is presented in Figure 9. The strongest peak in the power spectrum appears at

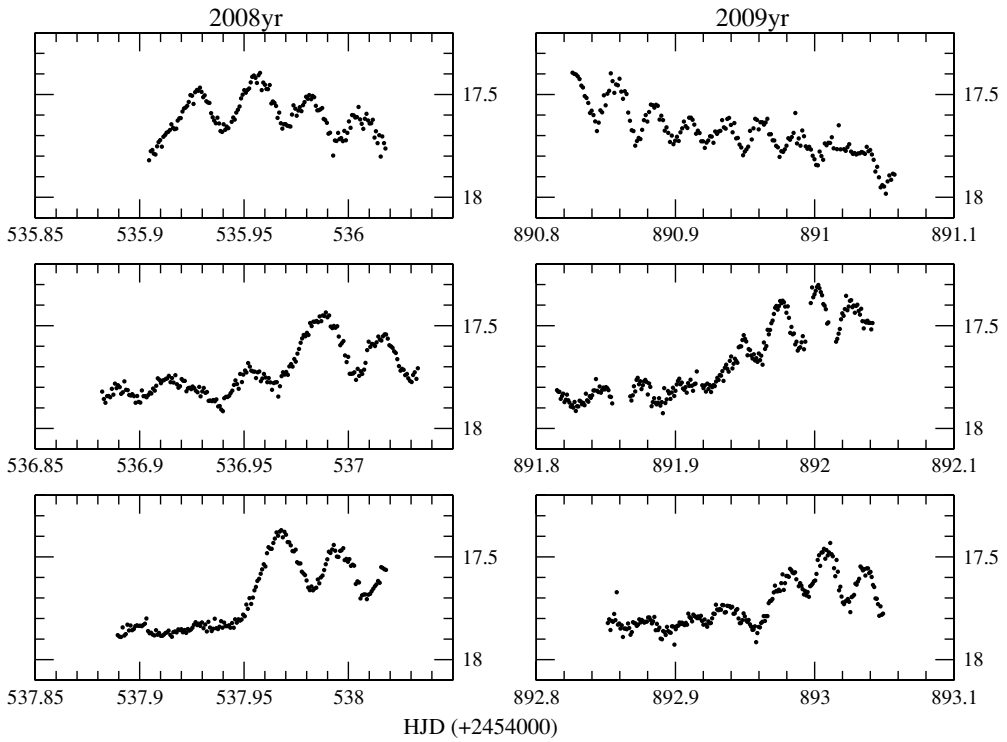

Figure 6. Light curve of SDSS 1238 in the *V* band obtained in 2008 and 2009 yy. Each night is presented in a separate panel.

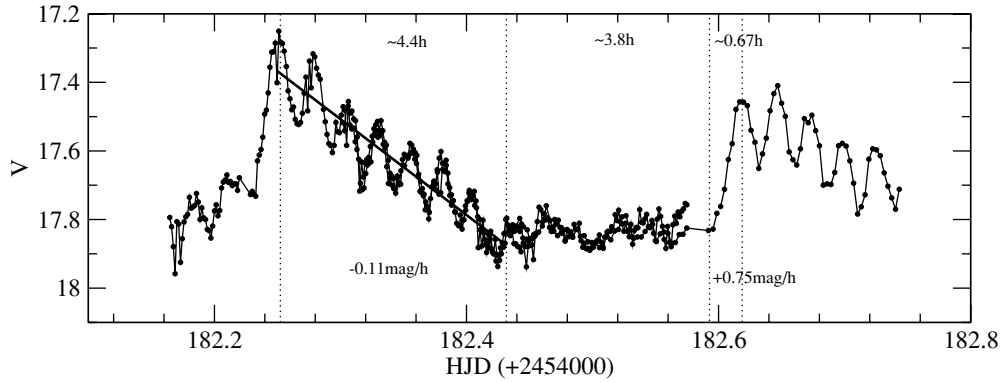

Figure 7. Light curve of SDSS 1238 in the *V* band obtained during about 15 hr continuous observations in HJD 2454182. Vertical dashed lines select different phases of the long-term variability (LTV). The numbers in the top of the figure are approximate durations for each marked phase of LTV and the numbers in the bottom are corresponding rates of the magnitude change during fading and increasing of the object brightness.

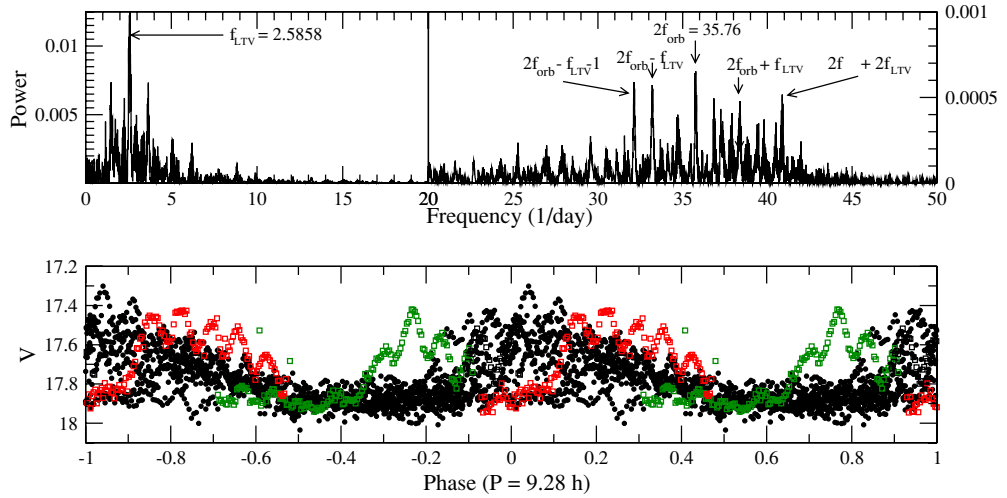

Figure 8. Top: the power spectrum of all the photometric data presented in the top panel of Figure 5. Bottom: the light curve comprised of all the data folded on $P = 9.28$ hr. The open color points show brightenings with maximal displacement in the light curve folded on $P = 9.28$ hr.

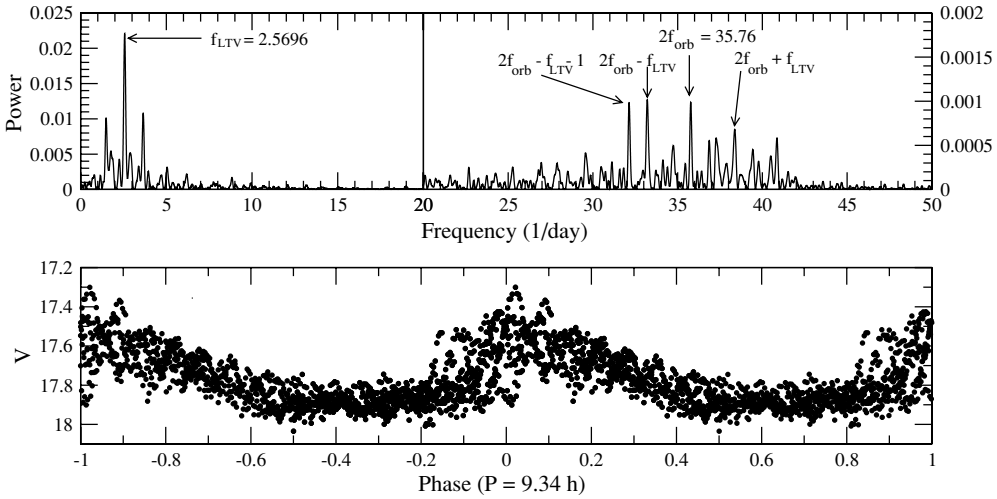

Figure 9. Top: the power spectrum of the data obtained in the period of HJD 2454177.1−2454185.6 (see Figure 5). Bottom: the light curve comprised of the selected data from the period of HJD 2454177.1−2454185.6 folded on $P = 9.34$ hr period.

a frequency corresponding to $P^{*}_{\rm LTV} = 9.34(26)$ hr. The light curve folded with this period is coherent during the considered time (Figure 9), i.e., macro-profile of the brightenings (the rise, the peak, the declining slope, and minimum duration) repeats itself with high accuracy and, if not for the high-frequency modulation also present in the light curve, the folded curves would concur. Combining the entire available data obtained during the 2004–2009 observational runs does not permit a determination of a single period with which the entire data set can be folded. Clearly, the LTV modulation is not strictly periodic, but probably maintains coherence in a timescale of several weeks and certainly has a cyclic nature.

The LTV (the brightenings) presents a fast rise in the object brightness of up to 0.4–0.6 mag, lasting about half the orbital period (∼0.7 hr) with the brightness falling back to the quiescence level during the next 4.4–4.6 hr (Figure 7). After that, the object remains in quiescence during about another 4 hr. The brightness increases at a rate of ∼0.75 mag hr^{-1}, and the falling rate is about ∼0.10 mag hr^{-1}. Sometimes, the rise in the brightness happens more slowly and lasts until almost one full orbital period (Figure 5 nights: 156, 179).

A short-term variability is clearly present during the brightenings. The amplitude of the short-term variability depends strongly on the phase of brightenings. The amplitude is larger then the total brightness increases and falls, sometimes practically disappearing, between the brightenings (Figures 5–7). Curiously, when the LTV is coherent, the signal at double orbital frequency decreases and a beat frequency between the LTV and $2 \times f_{\rm orb}$ becomes dominant in the range of frequencies around 36 cycles day^{-1}. Removing LTV has little effect, because this does affect the frequency modulation but not the amplitude modulation. The strong relation between LTV cycle coherence and the strength of $2 \times f_{\rm orb}$ modulation attests that these two phenomena are physically linked in more than a simple amplitude correlation. We suspect that the brightenings and formation of spiral arms in the disk are the result of the same process, but its cyclic nature remains unclear.

6. DISCUSSION AND CONCLUSIONS

In recent years, a number of objects were discovered, mostly thanks to the Sloan Digital Sky Survey (SDSS), which can be characterized as WZ-Sge-type CVs in quiescence, judging by their ∼80–85 minute periods, spectral appearance, and lack of SU UMa style outburst activity. Currently, there are about 20 objects with similar characteristics which were selected from the SDSS lists. Three such objects are GW Lib, V455 And, and SDSS 0804, which underwent a typical WZ-Sge-type superoutburst in 2006–2007, confirming the correct assessment of their nature from their behavior in quiescence. But unlike classical WZ-Sge stars, some of them differ by the presence of permanent double humps per orbital period in the light curve. The significance of the double-humped light curve lies in the assumption that it is produced by the spiral structure in the accretion disk. The spiral arms in accretion disks have been detected before by means of Doppler tomography in long-period systems only during DN outburst. We are not aware of any reports of double-humped light curves during these detections. Double-humped light curves have previously come to attention, as they were detected during superoutbursts of WZ-Sge. It was soon suggested that they are result of 2:1 resonance (Patterson et al. 2002a), as one of the possibilities. Also, spiral arms are formed in the accretion disk of the WZ-Sge undergoing superoutburst (Steeghs 2004), because, according to our hypothesis, WZ-Sge accretion disk reaches the resonance radius only during superoutburst. Nevertheless, the spiral structure has been observed persistently along with the double-humped light curve in two similar short-period systems, SDSS 0804 and SDSS 1238, in quiescence. We assume that the spiral structure formed in low viscosity, quiescent disks is a result of distortion of the disk by the 2:1 resonance. The 2:1 resonance may happen only in the accretion disk of a system with extreme mass ratio of $q \leqslant 0.1$. Such mass ratio is achieved only in systems known as bounce-back, or, in other words, systems which have reached a minimum period of ≈80 minutes and have turned to slightly longer periods according to Paczynski (1981). It is expected that bounce-back systems are numerous (Kolb & Baraffe 1999), but until recently very few candidates have been found. The SDSS helped to uncover a large number of new CVs, with interesting new features (Gänsicke et al. 2009). Among them, there is a number of short-period systems, some of which turned out to belong to the long-sought bounce-back system (Littlefair et al. 2008; Mennickent & Diaz 2002).

We have unveiled a brown dwarf secondary in SDSS 1238, probably as late as L4, thus providing strong evidence that this object is a real bounce-back system. We also estimated

parameters of the WD. The best fit to the SED converges if the primary is a massive $M_{\rm WD} \approx 1.0\,M_{\odot}$ WD with a $T_{\rm WD} = 12{,}000$ K temperature. Both numbers seem plausible since the system is very old and the WD is expected to be relatively massive and cool. These findings provide further support to our claim that by simply observing a permanent double-humped light curves one can identify an evolved, bounce-back system instead of using other complicated methods.

It is important to note that SDSS 1238 has another peculiarity, which Zharikov et al. (2006) termed brightenings. There was only one other system known to exhibit brightenings, namely, SDSS 0804, but since it underwent a superoutburst in 2006, its photometric behavior has drastically changed. The brightenings shortly detected by Szkody et al. (2006) in SDSS 0804 before the superoutburst have been replaced by: (1) the mini-outburst activity with permanent presence of the double-humped light curve of constant amplitude (Zharikov et al. 2008) and by (2) a 12.6 minute period, probably corresponding to pulsation activity of the WD (Pavlenko et al. 2007). Therefore, at present, SDSS 1238 is the only object known to show brightenings. It greatly complicates the study of this phenomenon. Based on new multi-longitude continuous monitoring, we demonstrated here that the brightenings are of cyclic nature with a recurrence time of $\approx$9 hr and they are probably coherent over several cycles. There seems to be a strong correlation between brightenings cycles and the amplitude of double-hump periodic variability. This is believed to be the result of spiral arms in the accretion disk of bounce-back systems with an extreme mass ratio, in which the accretion disk extends beyond a 2:1 resonance radius. The tomogram of a simulated accretion disk in the regime of resonance closely resembles the observed one and supports this hypothesis. The formation of a spiral structure in the disk can be accounted by the appearance of double humps in the light curve, but it cannot be the reason for increased brightness of the disk. The disk brightness directly depends on the mass transfer rate and its change should probably reflect change in mass transfer. No explanation is readily available as to why that rate can be variable and cyclical, but possible speculations include counteraction (1) to the heating of the secondary by brightenings, or (2) to tidal interaction between the secondary with the resonance attaining accretion disk.

This work was supported in part by DGAPA/PAPIIT IN109209 and IN102607, and CONACYT 59732 projects.

REFERENCES

Baba, H., et al. 2002, PASJ, 54, L7
Close, L. M., et al. 2003, ApJ, 587, 407
Deeming, T. J. 1975, Ap&SS, 36, 137
Gänsicke, B. T., et al. 2009, MNRAS, 397, 2170
Heemskerk, M. H. M. 1994, A&A, 288, 807
Howell, S. B., Adamson, A., & Steeghs, D. 2003, A&A, 399, 219
Knigge, C. 2006, MNRAS, 373, 484
Kolb, U., & Baraffe, I. 1999, MNRAS, 309, 1034
Kunze, S., & Speith, R. 2005, in ASP Conf. Ser. 330, The Astrophysics of Cataclysmic Variables and Related Objects, ed. J. M. Hameury & J. P. Lasota (San Francisco, CA: ASP), 389
Kunze, S., Speith, R., & Riffert, H. 1997, MNRAS, 289, 889
Kurucz, R. 1993, ATLAS9 Stellar Atmosphere Programs and 2 km/s grid, Kurucz CD-ROM No. 13 (Cambridge, MA: Smithsonian Astrophysical Observatory), 13
Lin, D. N. C., & Papaloizou, J. 1979, MNRAS, 186, 799
Littlefair, S. P., Dhillon, V. S., Marsh, T. R., Gänsicke, B. T., Southworth, J., Baraffe, I., Watson, C. A., & Copperwheat, C. 2008, MNRAS, 388, 1582
Lynden-Bell, D. 1969, Nature, 223, 690
Matsuda, T., Sekino, N., Shima, E., Sawada, K., & Spruit, H. 1990, A&A, 235, 211
Martini, P., Persson, S. E., Murphy, D. C., Birk, C., Shectman, S. A., Gunnels, S. M., & Koch, E. 2004, Proc. SPIE, 5492, 1653
Marsh, T. R., & Horne, K. 1988, MNRAS, 235, 269
McLean, I. S., McGovern, M. R., Burgasser, A. J., Kirkpatrick, J. D., Prato, L., & Kim, S. S. 2003, ApJ, 596, 561
McLean, I. S., Prato, L., McGovern, M. R., Burgasser, A. J., Kirkpatrick, J. D., Rice, E. L., & Kim, S. S. 2007, ApJ, 658, 1217
Mennickent, R. E., & Diaz, M. P. 2002, MNRAS, 336, 767
Murray, J. R. 1996, MNRAS, 279, 402
Nauenberg, M. 1972, ApJ, 175, 417
Ogilvie, G. I. 2002, MNRAS, 330, 937
Paczynski, B. 1981, Acta Astron., 31, 1
Patterson, J., et al. 2002a, PASP, 114, 721
Patterson, J., et al. 2002b, PASP, 114, 1364
Pavlenko, E., et al. 2007, in ASP Conf. Ser. 372, 15th European Workshop on White Dwarfs, ed. R. Napiwotzki & M. R. Burleigh (San Francisco, CA: ASP), 511
Persson, S. E., Murphy, D. C., Krzeminski, W., Roth, M., & Rieke, M. J. 1998, AJ, 116, 2475
Piskunov, N. E. 1992, Stellar Magnetism, ed. Yu. V. Glagolevskij & I. I. Romanyuk (St. Petersburg: NAUKA), 92
Sawada, K., Matsuda, T., & Hachisu, I. 1986a, MNRAS, 221, 679
Sawada, K., Matsuda, T., & Hachisu, I. 1986b, MNRAS, 219, 75
Steeghs, D. 2001, Astrotomography, Indirect Imaging Methods in Observational Astronomy (Lect. Notes in Physics 573), ed. H. M. J. Boffin, D. Steeghs, & J. Cuypers, 45
Steeghs, D. 2004, RevMexAA Conf. Ser., 20, 178
Steeghs, D., & Stehle, R. 1999, MNRAS, 307, 99
Stehle, R. 1999, MNRAS, 304, 687
Szkody, P., et al. 2003, AJ, 126, 1499
Szkody, P., et al. 2006, AJ, 131, 973
Southworth, J., Gänsicke, B. T., Marsh, T. R., de Martino, D., Hakala, P., Littlefair, S., Rodríguez-Gil, P., & Szkody, P. 2006, MNRAS, 373, 687
Tinney, C. G., Burgasser, A. J., & Kirkpatrick, J. D. 2003, AJ, 126, 975
Truss, M. R. 2007, MNRAS, 376, 89
Warner, B. 1995, Cambridge Astrophysics Series, Vol. 28 (Cambridge: Cambridge Univ. Press)
Zharikov, S. V., Tovmassian, G. H., Napiwotzki, R., Michel, R., & Neustroev, V. 2006, A&A, 449, 645
Zharikov, S. V., et al. 2008, A&A, 486, 505